Journal of Information Systems Engineering and Management
2025, 10(11s)
e-ISSN: 2468-4376
https://www.jisem-journal.com/

Research Article

Development of a Deep Mask Region-Based Convolutional Neural Network with Improved Weighted Quantum Wolf Optimization for Sickle Cell Anaemia Detection and Classification

[1]Arularasi Peter* and [2]B. Pushpa
[1]*Research Scholar, Department of Computer and Information Science, Faculty of Science, Annamalai University, Tamilnadu, India, Email: arularasipeter@gmail.com*
[2]*Assistant Professor, Department of Computer and Information Science, Faculty of Science, Annamalai University, Tamilnadu, India, Email: Pushpasidhu@gmail.com*
**Corresponding Author Email: arularasipeter@gmail.com*

ARTICLE INFO

Received: 16 Nov 2024

Revised: 22 Dec 2024

Accepted: 10 Jan 2025

ABSTRACT

To effectively manage Sickle Cell Anaemia (SCA), a severe inherited blood condition, early detection and accurate categorization are essential. Timely and precise identification is hindered by the high error rates, limited scalability, and dependency on personal expertise associated with conventional diagnostic approaches. To address these challenges, this study proposes a novel Deep Mask Region-Based Convolutional Neural Network (DMRCNN) combined with Improved Weighted Quantum Wolf Optimization (IWQWO) for SCA identification and classification. By leveraging advanced feature extraction and segmentation methods, the DMRCNN enables precise localization and identification of abnormal cells in blood smear images. The IWQWO method optimizes the DMRCNN's hyper parameters enhancing the network's efficiency by achieving an optimal balance between convergence speed and prediction accuracy. The primary objectives of this study are to improve classification accuracy, reduce computational overhead, and minimize false positives and false negatives in SCA diagnostics. Experimental results demonstrate that the proposed system achieves 96.8% precision, 97.2% accuracy, 96.5% recall and 96.8% F1-score, surpassing existing approaches with superior metrics. These findings underscore the effectiveness of the proposed method in automating SCA detection and classification, paving the way for potential integration into clinical workflows for accurate and timely assessments.

Keywords: Sickle Cell Anaemia, Deep Mask Region-Based Convolutional Neural Network, Improved Weighted Quantum Wolf Optimization, Blood Smear Image Analysis, Hyperparameter Optimization, Medical Image Classification, Automated Diagnosis, Feature Extraction

1. INTRODUCTION

Sickle cell genes affect haemoglobin, a vital protein in blood. Individuals with sickle cell genes produce an abnormal Haemoglobin (HbS), normal Haemoglobin (HbA) [1]. It causes RBC to change into a sickle or crescent-moon shape leading to the characteristic symptoms of the condition. Individuals with SCA or sickle cell trait produce HbS is responsible for the condition. The presence of HbS causes normal RBC are typically soft and round to change into a rigid, sickle or crescent-moon shape [2]. The initial step in diagnosing SCA involves a blood test to analyse the sample for abnormalities. This preliminary examination, often referred to as a quick sickling test, serves as the foundation for further detailed investigations based on clinical requirements [3].

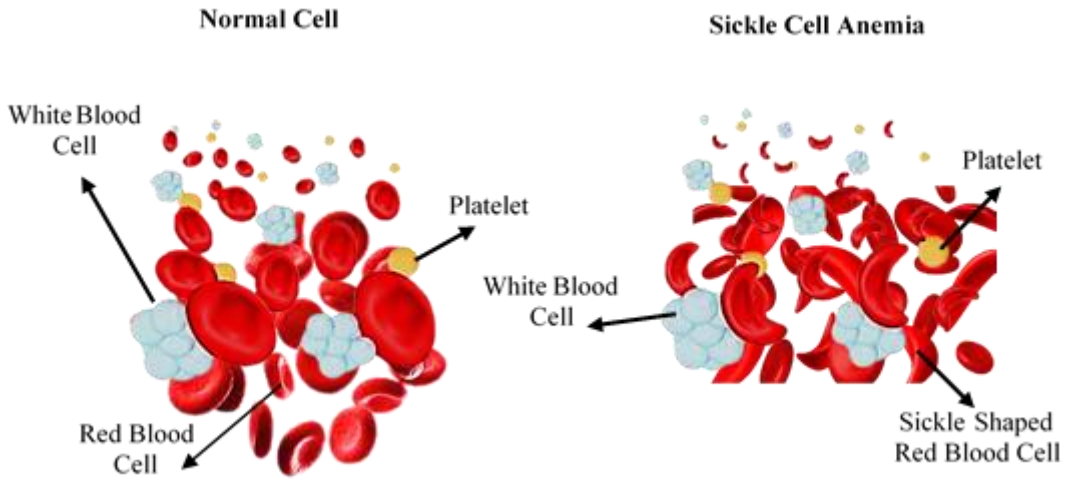

Figure 1: Biological illustration of the Sickle Cells

A person's diagnosis can determine whether they are homozygous or heterozygous for sickle cell genes. Sickle cell genes are inherited from parents and passed on to their offspring. If a family member has severe Sickle Cell Disease (SCD), a child may inherit the condition and develop sickle cell traits [4]. A person with the sickle cell trait is considered heterozygous carry one normal gene and one sickle gene. If both parents carry the sickle gene, their child has a chance of being homozygous (inheriting two sickle genes and having SCD), heterozygous (inheriting one sickle gene and one normal gene, resulting in the sickle cell trait), or normal (inheriting no sickle genes) [5].

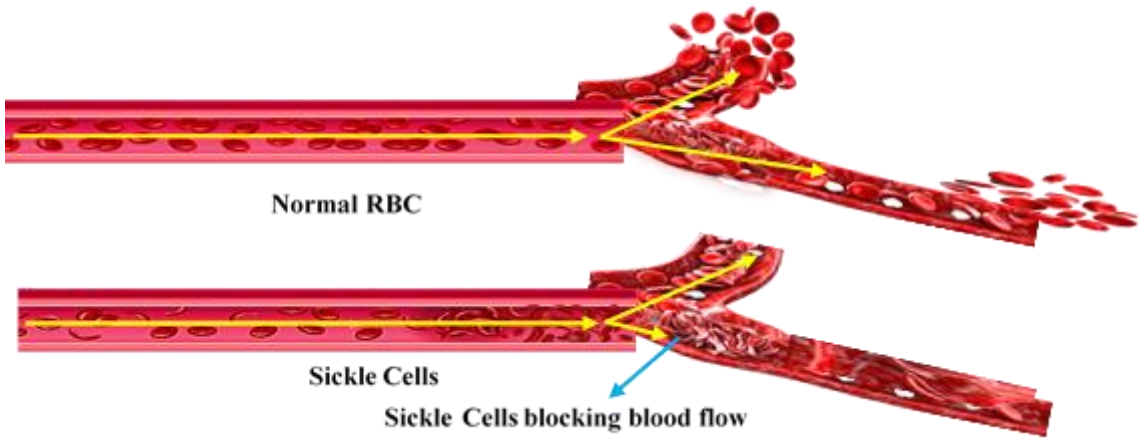

Figure 2: Blood Flow of Sickle Cells

As shown in Figure 2, normal blood flow efficiently delivers oxygen through the bloodstream without obstruction. Sickle-shaped RBC can become lodged in blood vessels, causing blood circulation to stop [6]. Although initially identified in the Black community, SCD has since been discovered in individuals from diverse ethnic groups, including those from Italy, Greece, the Mediterranean region, parts of the Middle East, and Central India. Early treatments for SCD include bone marrow transplants, blood transfusions, and antibiotics [7]. Many physicians recommend regular blood transfusions every one to two months, while antibiotics are used to manage risks such as chronic infections and pain. SCD is now identifiable in new-borns as a rare blood disorder marked by the presence of sticky, rigid, crescent-shaped RBC that adhere to one another [8].

Over time, damage caused by SCD can spread from a single organ to the entire body, potentially resulting in life-threatening complications. Early and prompt treatment, such as blood transfusions, is critical to preventing severe outcomes. The condition is caused by two faulty genes leading to the accumulation of HbS in the affected individual. Early detection of SCD is essential to reducing morbidity and mortality [9]. Several medical tests such as haemoglobin electrophoresis, sickle cell screening, and complete blood counts can identify haematological disorders by analysing the shape of RBC and haemoglobin profiles. These procedures require skilled personnel and well-equipped

laboratories can be challenging to establish in regions with limited medical infrastructure. While there is currently no definitive cure for SCD, treatments such as hydroxyurea, bone marrow transplants, and emerging gene therapies help manage symptoms, reduce complications, and alleviate pain [10].

In complete knee and hip replacements and cardiac surgeries, it was found that incorporating patient blood management significantly reduced transfusions, hospital stays, morbidity, and hospital readmissions. The safety of implementing patient blood management across an entire hospital was evaluated in a multi-center study [11, 12].

Low hemoglobin levels, the most common hematological disorder affect over two billion people globally. Early detection is critical for addressing serious causes of anaemia such as severe gastrointestinal bleeding. Anaemia is often challenging to diagnose through simple medical records or basic tests, and its consequences become evident when left unaddressed [13]. Comprehensive laboratory blood tests remain one of the most widely used methods for diagnosing anaemia. Advancements in deep learning algorithms now enable automatic feature extraction and one-shot classification offering potential improvements in anaemia detection and diagnosis [14].

The literature presents several methods for identifying SCA in red blood smears. Proposed novel computational imaging techniques capable of automatically recognizing SCA in RBC samples. The image dataset was obtained using camera-attached microscopy. Segmented images and clustering methods were applied to identify sickle cells and erythrocytes in the microscopic smears [15]. The efficacy of the proposed method was not fully evaluated, as key modern success metrics were not utilized. Superior clustering techniques were not compared to methods like fuzzy c-means and k-means clustering. Developed an ensemble ML algorithm to assess the severity of SCA among children with the condition. Simulation-based research demonstrated the algorithm's effectiveness in predicting eight different forms of SCD [16]. Classification reliability of the technique requires improvement. Introduced a fuzzy logic-based predictive framework to identify and evaluate SCA infection. Their prediction model utilized three input variables: the individual's genotype, fetal hemoglobin levels, and the severity of anaemia. The effectiveness of this framework, however, was not thoroughly evaluated [17]. To detect SCA, conducted comparative research using blood specimen images and various ML simulations. This study highlighted the potential of ML algorithms in identifying SCA but underscored the need for further optimization and validation [18]. Preparatory tasks were conducted to eliminate noise and enhance the quality of grayscale images, transforming them into high-quality formats. Artificial intelligence algorithms were employed to classify the images into sickle cells and normal cells. ML models under investigation demonstrated low efficiency indicating the need for the development of more robust and high-performing systems [19].

1.1 Problem Statement

For the illness to be effectively treated and managed, initial and accurate identification is essential. Existing diagnostic techniques often rely on the manual analysis of blood smear images, which is labour-intensive, prone to human error, and dependent on the expertise of healthcare professionals. Issues such as low precision, high rates of false positives and false negatives, and inadequate handling of unbalanced datasets are common challenges with conventional machine learning and deep learning approaches. These limitations hinder the timely and accurate detection of SCA, particularly in medical facilities with limited resources. To enhance clinical decision-making, there is an urgent need for a reliable, automated, and efficient system capable of precisely identifying and categorizing SCA from blood smear images. The proposed system should aim to optimize both diagnostic accuracy and computational performance.

1.2 Motivation

SCA is becoming increasingly prevalent globally, particularly in regions with limited resources. This underscores the urgent need for innovative diagnostic approaches. Conventional diagnostic techniques, such as manual blood smear assessments, are time-consuming, labour-intensive, and often yield unreliable results due to human errors. The challenges of timely and accurate SCA identification are exacerbated by the limitations of current computerized methods, which suffer from low accuracy and processing inefficiencies. A promising solution to these challenges lies in the rapid advancement of deep learning and optimization techniques. By combining advanced image processing with intelligent optimization methods, an effective, adaptable, and accurate diagnostic system can be developed. The potential to revolutionize SCA identification and categorization, reduce the workload for healthcare providers, and improve patient outcomes through timely and accurate diagnosis especially in areas with limited medical facilities and expertise is the primary motivation behind this research.

2. RELATED WORKS

SCA underscores the importance of a comprehensive disease diagnosis involves precise anomaly detection and classification key elements for the accurate diagnosis, treatment planning, and evaluation of treatment outcomes for SCD. The accuracy and reliability of sickle cell detection improve when complex groups of cells are effectively separated [20]. Cell morphology plays a vital role in identifying sickle cells significantly differ in structure from normal blood cells. To detect stationary objects in images, proposed a pixel classification method that uses segmentation techniques. These objects are then tracked using a new approach called adaptable edge orientations. This method shows a 95% efficiency in object recognition, outperforming current best practices [21]. Examined the principles for evaluating the efficacy of change detection systems in their investigation of various image change detection techniques. To improve detection accuracy when processing aerial images developed an object detection method using a specialized Deep Neural Network known as Feature Fusion Deep Networks (FFDN). This method not only enhances the geographical connection between high-density objects but also improves hierarchical representations [22]. Manual thresholding chosen using a limited number of execution trials or prior knowledge, is typically ineffective in reliably separating the intended object from healthcare imaging. In contrast, personalized thresholding methods are more accurate because they autonomously predict the threshold level based on the image data [23].

The edge data within the image is used to determine the threshold values in an edge-based reduction method. Examples of such methods include Sobel, Canny, and Laplacian edge detection. For Laplacian edge detection, the threshold setting is primarily determined by the derivative information related to pixel brightness. The potential edge identification of the Canny edge detection technique is based on the magnitude of gradient data. In contrast, compression relies on non-maximal suppression and hysteresis thresholding [24]. Employed Sobel edge detection to detect sickle cells in RBCs. Focus on high spatial frequency to locate the boundaries. In sickle cell detection, segmentation is a crucial step, where the gradient's amplitude at each pixel is calculated. The changing slope of the area's boundaries is important in the region-based threshold approach [25]. Bone marrow defects, malnutrition, and various disorders can cause a significant decrease in blood sugar levels [26]. Anaemia, a dangerous haematological disorder can lead to symptoms such as mood swings, cognitive decline, pallor, and physical weakness. In severe cases, it may even cause heart attacks. World Health Organization (WHO) classifies anaemia as a particularly hazardous condition for infants and pregnant women. The most common way to diagnose anaemia and monitor Hb levels is through invasive blood tests [27].

These tests are uncomfortable and carry a risk of infection, particularly when performed in a hospital setting. These tests should be performed by a qualified healthcare professional who can accurately interpret the visual signs in relation to anaemia. Additional risks associated with manual examination include human error, non-reproducible results, and bias among observers [28,29]. The proposed combinations aim to reduce human errors caused by fatigue or infirmity by utilizing medical data for diagnoses. This approach demonstrates inefficiency and failure in certain contexts. SCA is now a global haematological disorder that requires prompt medical intervention. Describe the history of SCD both in India and globally and provide an overview of its symptoms, warning signs, consequences, and course of treatment [30]. The blood cells of individuals with SCD and thalassemia are classified using blood features. To reduce the time and resources needed for managing SCD complex control systems, this work employs a Multilayer Perceptron (MLP) to more accurately model the condition. Simulation results show that the MLP classifier predicts SCD and thalassemia with a precision of 99.9% [31]. Due to the computational requirements of the MLP method, it is not suitable for use by regular medical lab staff in time-sensitive clinical scenarios. Proposed using artificial intelligence to predict and estimate haemoglobin levels based on haematological criteria [32]. SCA is a serious haematological disorder that often requires hospitalization and can be fatal. Present a two-step process: first, automated RBC removal from blood test images to identify the RBC Region of Interest (ROI) [33]. Deep learning AlexNet system is used to classify and predict abnormalities in individuals with SCA. Classified blood smear microscopic images into sickle cells, dacryocytes, and ovalocytes using the k-nearest neighbor (k-NN) technique [34]. After several pre-processing steps, including noise reduction with a median filter, the images were segmented. Although the proposed method worked well on the images only 100 images were used for training and evaluation, raising concerns about its generalizability. Analysed medical records of SCD patients using ML and natural language processing techniques. In their study, the researchers used their knowledge of sickle cell conditions to focus on patient information, pain, emotional distress, and pain scores [35].

2.1 Research Gap

Accurately identifying and classifying SCA is still difficult, even with improvements in automated medical image processing. The majority of approaches are unable to properly optimize hyper parameters results in less than-ideal performance of models and higher computational expenses. For accurate diagnosis, existing techniques for optimization for model tuning are neither strong nor flexible enough to handle complicated information from medical imaging. Combining deep learning models with sophisticated optimization techniques to improve SCA identification precision and effectiveness. To improve the general efficacy of automatic SCA detection techniques, these gaps underscore the need for a new hybrid method that tackles the issues of feature extraction, diagnostic reliability, and hyperparameter optimization.

3. MATERIALS AND METHODS

To accurately detect and classify SCA, this study focuses on developing an innovative structure that combines an IWQWO algorithm with a DMRCNN shown in Figure 3. The DMRCNN is designed to utilize cutting-edge deep learning algorithms for precise segmentation and feature extraction from blood smear images enabling the accurate detection of abnormal RBCs. By fine-tuning the DMRCNN's hyper parameters such as learning rate, filter size, and network depth, IWQWO method enhances efficiency while maintaining a balance between diagnostic precision and computational effectiveness.

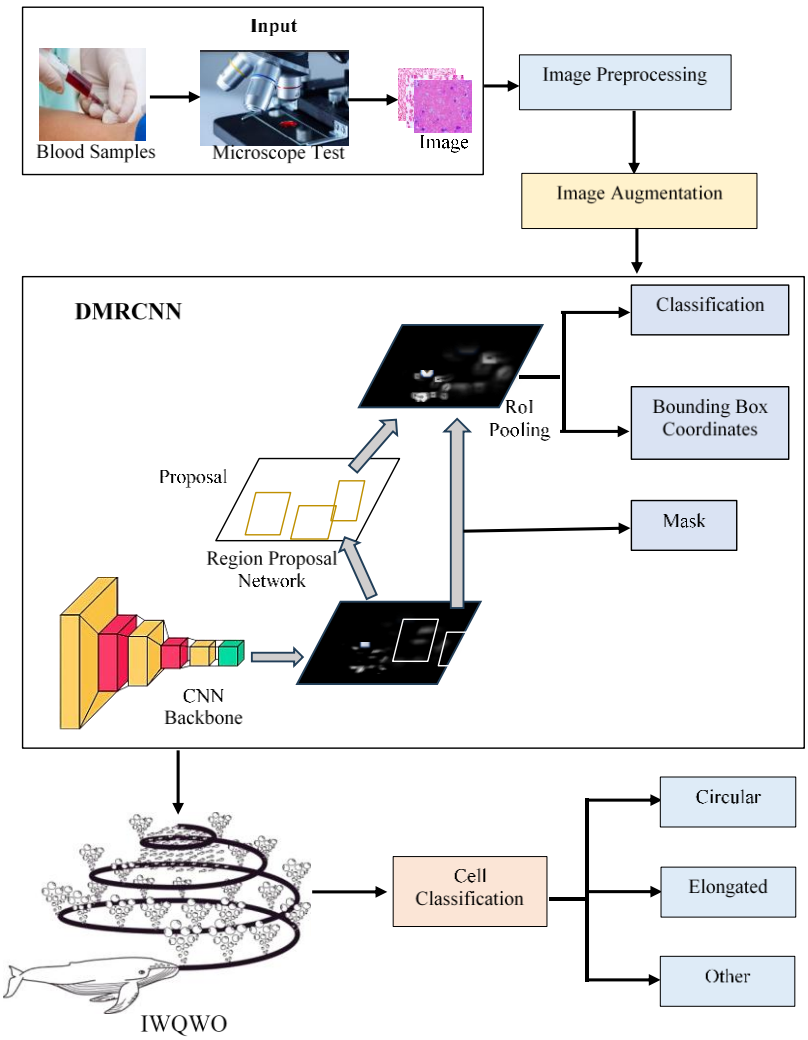

Figure 3: Proposed Architecture

This hybrid technique addresses critical issues in SCA identification, reducing computational costs, improving generalization, and minimizing false positives and negatives. The proposed model outperforms existing methods, as demonstrated by comprehensive experimental analysis show improved metrics in precision, accuracy, recall, and F1-

score. Considering the potential to improve early diagnosis and patient outcomes in both clinical and resource-constrained settings, this study advances reliable and scalable computerized diagnostic methods for SCA.

3.1 Dataset description

High-resolution microscopic blood smear images constitute the dataset used for the identification and classification of SCA, as shown in Table 1. The dataset contains a total of 10,000 images, evenly split between two classes: normal RBCs and sickle-shaped cells. To ensure accurate labelling, haematological specialists annotate the images, using masks for segmentation or bounding boxes to highlight areas of interest. To maintain consistency, the images are provided in common file formats, such as JPEG or PNG, with a fixed resolution of 256 x 256 pixels. When available, additional contextual information for research purposes can be included, such as patient ID, age, and medical diagnosis. The dataset is divided into 80% training data, 20% testing data, and 10% validation data for model development and evaluation. This well-structured dataset ensures efficient and reliable SCA identification, facilitating robust training, hyper parameter tuning, and accurate assessment of the proposed model. Sample datasets is shown in Table 2.

Table 1: Dataset Description

Attribute	Description	Value/Range
Dataset Name	Sickle Cell Blood Smear Images	-
Source	Publicly available medical image repositories or hospital-collected data	-
Image Type	Microscopic blood smear images	RGB, Grayscale
Total Images	10,000 (for example)	-
Resolution	High resolution (e.g., 256x256 pixels)	Fixed or variable
Classes	Normal cells, Sickle-shaped cells	2
Class Distribution	Balanced (e.g., 50% normal, 50% sickle-shaped cells)	Equal/Imbalanced
Annotations	Manual annotations by hematology experts	Bounding boxes, cell segmentation
Preprocessing Steps	Resizing, normalization, noise removal, data augmentation (e.g., flipping, rotation, etc.)	Applied
Train-Test Split	80% training, 20% testing	Standard split
Validation Set	10% of training data	Used for hyperparameter tuning
File Format	JPEG, PNG	-
Metadata	Patient ID, Age, Gender, Clinical Diagnosis (if available)	Optional

Table 2: Sample data

Image ID	File Name	Class	Annotation Type	Bounding Box (x, y, w, h)	Patient Age	Patient Gender	Clinical Diagnosis
001	img001.png	Normal	Segmentation	-	26	Male	No abnormalities
002	img002.png	Sickle Cell	Bounding Box	(45, 60, 30, 30)	19	Female	Sickle Cell Anemia

003	img003.png	Sickle Cell	Bounding Box	(70, 80, 40, 40)	33	Male	Sickle Cell Anemia
004	img004.png	Normal	Segmentation	-	30	Female	No abnormalities
005	img005.png	Sickle Cell	Bounding Box	(30, 50, 25, 25)	22	Male	Sickle Cell Trait

People with SCD at the General Hospital in Chennai provided blood samples with RBC images. 66 of the 196 images shows various cells that have been classified as circular (202), elongated (211), or deformed in some other way (213). The dimension of each cell is 80 × 80 pixels. The results generated by the methods employed to categorize the cells in the RBC images were validated using the doctor's requirements, a specialized method. Figure 4 displays the dataset's particular cell samples.

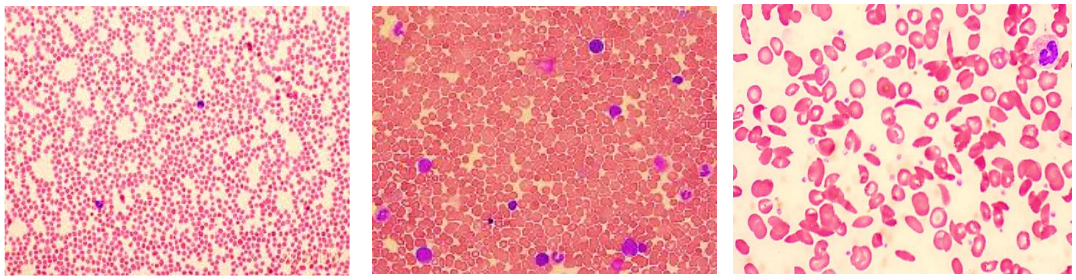

Figure 4: Images of healthy and Unhealthy SCA

3.2 Image Pre-processing

A crucial step in improving the caliber of input information for artificial intelligence models is image pre-processing. Common preliminary processing methods for standardizing, cleaning, and preparing blood smear images shown in Figure 5.

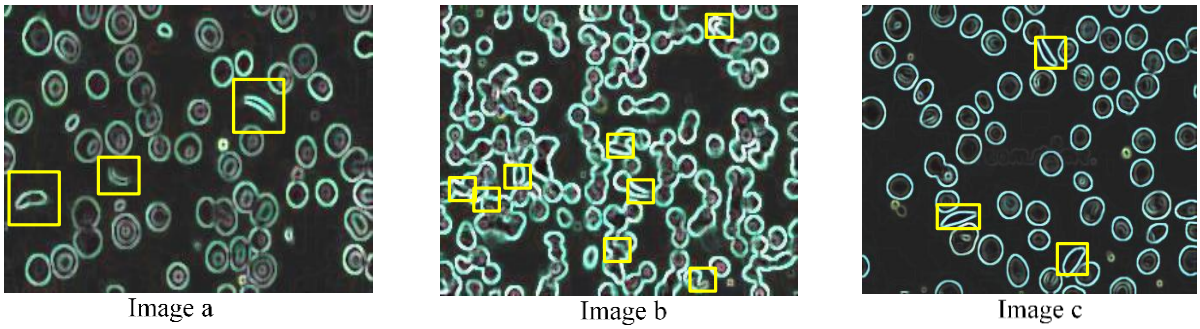

Figure 5: Pre-processed image

Image Resizing: Resizing ensures that all input images have a consistent size. For example, resizing images to N * N dimensions (e.g., 256 x 256) can be represented as:

$$X'(i',j') = X\left(\frac{i}{N_i} \times N, \frac{j}{N_j} \times N\right) \quad (1)$$

Where: $X(i,j)$ Original image. $X'(i',j')$ Resized image. N_i, N_j Original dimensions. N: Target dimension.

Normalization: It scales pixel intensity values to a range of [0, 1] or [-1, 1], which helps accelerate convergence in deep learning models. For an image X with pixel values P, the normalized pixel values P' are computed as:

$P' = \frac{P - P_{min}}{P_{max} - P_{min}}$ (2)

Where: P_{min} Minimum pixel value (usually 0). P_{max} Maximum pixel value (usually 255 for 8-bit images).

Noise Removal (Gaussian Filtering): To reduce noise, a Gaussian filter is applied:

$G(i,j) = \frac{1}{2\pi\sigma^2} exp\left(-\frac{i^2+j^2}{2\sigma^2}\right)$ (3)

The convolution operation between the image X and the Gaussian kernel $G(i,j)$ is:

$X'(i,j) = X(i,j) * G(i,j)$ (4)

Where * represents convolution, and σ is the standard deviation of the Gaussian kernel.

Z-Score Normalization: Standardizes the image by centering pixel values around the mean with unit variance:

$P' = \frac{P - \mu}{\sigma}$ (5)

Where: P: Original pixel value. μ: Mean of all pixel values in the image. σ: Standard deviation of all pixel values.

Data Augmentation (Rotation, Scaling, Flipping): To increase dataset variability:

Rotation: Rotate the image by θ using affine transformations: $\begin{bmatrix} i' \\ j' \end{bmatrix} = \begin{bmatrix} cos\theta & -sin\theta \\ sin\theta & cos\theta \end{bmatrix} \begin{bmatrix} i \\ j \end{bmatrix}$ (6)

Scaling: Scale the image by a factor s: $i' = s.i,\ j' = s.j$ (7)

Flipping: Flip the image horizontally or vertically: $i' = W - i\ or\ j' = H - j$ (8)

Where W, H are the width and height of the image.

Histogram Equalization: It enhances contrast by redistributing intensity levels:

$P' = CDF(P) \times (L - 1)$ (9)

Where: CDF(P): Cumulative distribution function of pixel intensities. L: Number of intensity levels (e.g., 256 for 8-bit images).

Binarization: Convert the image to a binary format to segment regions of interest:

$P' = \begin{cases} 1\ if\ P \geq T \\ 0\ if\ P < T \end{cases}$ (10)

Where T is the threshold value.

3.3 Feature extraction using DMRCNN

The initial stage's responsibilities included creating proposals and scanning images shown in Figure 6. The following phase's objectives included classifying objects, generating masks for every RBC in the quantitative portion of the image, and generating bounding box coordinates. High-level characteristics of the image were extracted via propagation backward featured pyramid networks with DMRCNN foundation. On the validation data set, the angle of Intersection over Union (IoU) of masking and the categories cross-entropy of categorization were computed to track the effectiveness of segments and categorization, correspondingly.

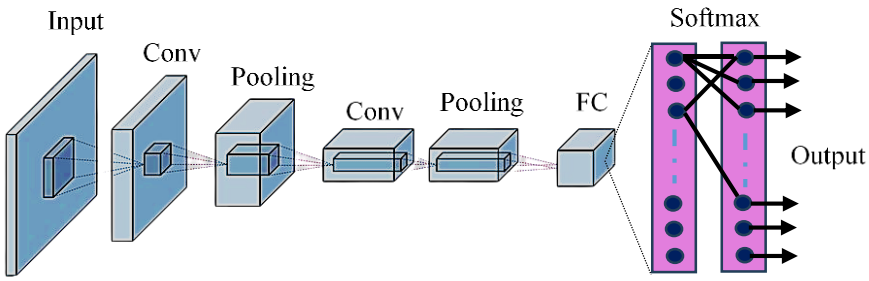

Figure 6: DMRCNN model for SCA detection

DMRCNN combine CNNs with region-based suggestions for obtaining characteristics at different degrees of conceptualization is particularly helpful for detection of SCD. Convolutional layers in DMRCNN gather spatial characteristics when suggestions for regions concentrate on areas of concern.

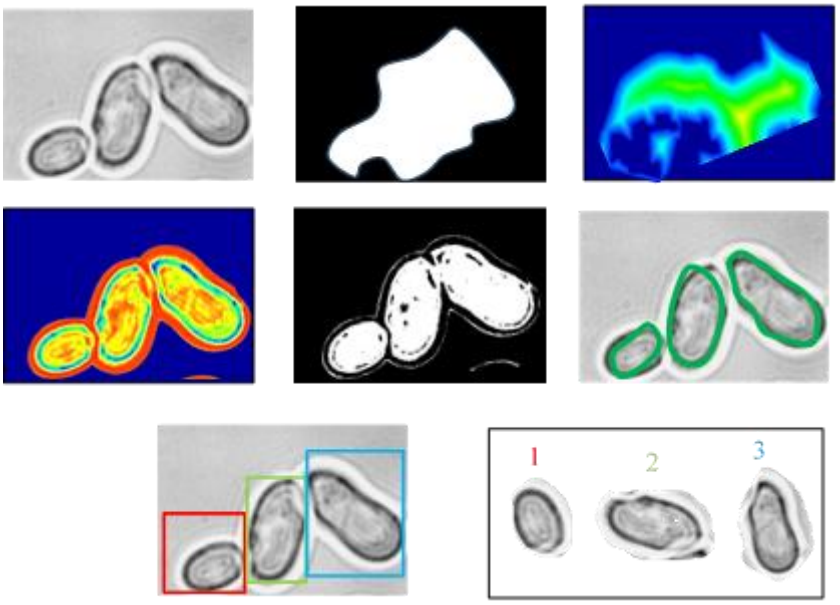

Figure 7: (a) ROI patch; (b) binary ROI mask image; (c) Transform results using Euclidean distance (d) Random walk with probability map (e) RBC binary mask separated (f) RBC outlines segmented (g) Single RBC with bounding box (h) Single RBC patches

Matching bounding boxes of the ROI, the sub-images in the two boxes were produced is shown in Figure 7. Successfully eliminated overlapped RBCs using DMRCNN. As a result, touching RBC separating issue by using the separation transformation and the random walking approach to create the RBC border. This technique may automatically determine the RBC seed locations. Figure 7 illustrates the precise separating process.

3.4 Improved Weighted Quantum Wolf Optimization

The Quantum Whale Optimization Algorithm (QWO) is an optimization system influenced by nature that imitates whale hunting tactics. The humpback whales bubble-net eating habits served as the model for the computer program. Finding the best answers to issues related to optimization is meant to be analogous to the organic method of bubble-net hunting, in which whales produce a sequence of bubbles to catch fish. An enhanced variant of QWO called IWQWO uses quantum technology and balanced variables to increase the method's capacity. To better investigate the search field enhancing the utilization phase, the enhancement usually including weights in the analysis stage and incorporating quantum operations. An enhanced variant of the classic WOA is called IWQWO. The main purpose of the WOA is to solve optimization issues by simulating the bubble-net hunting actions of humpback whales shown in Figure 8. Two significant improvements are introduced by the IWQWO:

Weighted Mechanism: To equalize exploring (finding new regions) and exploiting (fine-tuning the best-found solution) during the procedure of optimization, adaptable weights are added to the location update formulas.

Quantum Mechanism: The method uses quantum-based randomization, which was motivated by the theory of quantum mechanics, to improve exploration and avoid early convergence to optimal local conditions.

The purpose of these enhancements is to enhance outcomes for challenging optimization issues and overcome the shortcomings of the existing WOA.

A powerful method of optimization called IWQWO can greatly enhance the accuracy of models when used for choosing characteristics in the identification of SCD. The approach guarantees the effective use of hardware and software and improves the accuracy of diagnosis of artificial intelligence algorithms for SCA by carefully choosing the most pertinent characteristics.

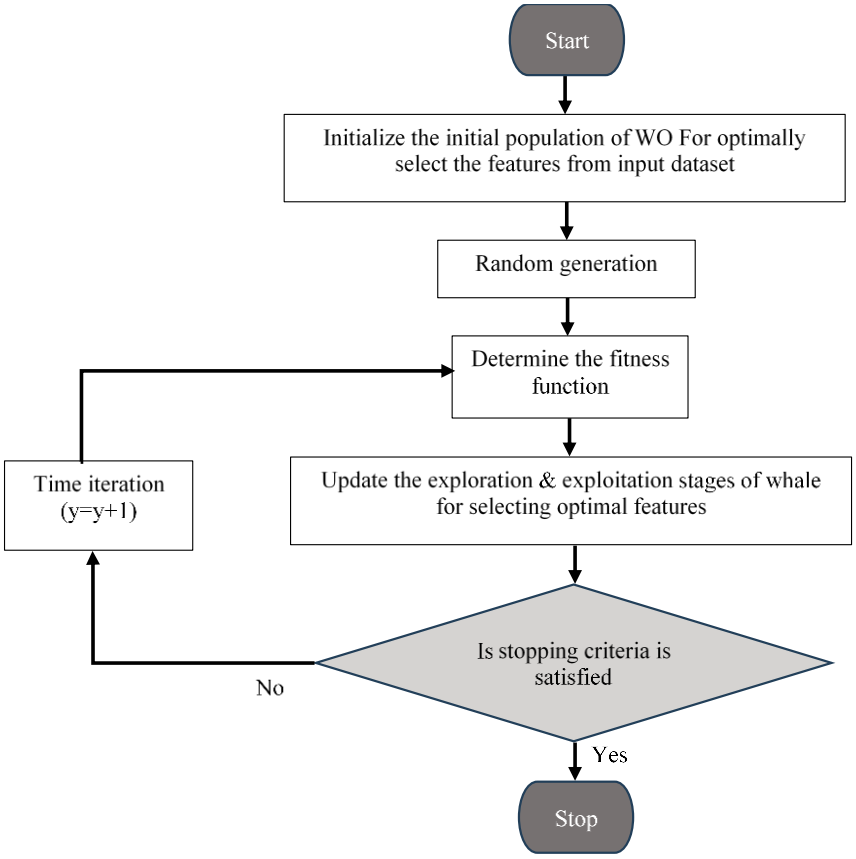

Figure 8: Flow chart of IWQWO algorithm for optimally selects the features from input dataset

3.5 Cell Classification for SCA Detection Based on the Proposed System

Using characteristics taken from cell pictures or blood test outcomes, the cell categorization procedure in SCA diagnosis seeks to categorize blood cell specimens as either sickled or healthy. Healthcare providers can use a classification approach to effectively diagnose sickle cells by using the DMRCNN with the IWQWO for choosing characteristics. Characteristics including cell area, structure, and abnormalities characteristic of sickled RBC are all recognized by the DMRCNN structure for cell categorization. To extract extremely fine characteristics and forecast the cardiovascular cell class (normal or sickled), it makes use of fully convolutional layers of data and region-based masking forecasts.

Step 1: Whale Position Update in WOA (Original)

In the classical WOA, the update equation for the whale's position is given by:

$$I^{(t+1)} = I^{(t)} + \alpha.rand(0,1).\left(P - I^{(t)}\right) + \beta.rand(0,1).(G - I^{(t)}) \quad (11)$$

Where: $I^{(t)}$ is the current position of the whale at iteration t, P is the personal best position of the whale, G is the global best position of the population, α and β are parameters controlling the influence of personal and global best positions on the new position, rand(0, 1) is a random number generated in the range [0, 1].

Step 2: Weighted Position Update in IWQWO

In IWQWO, adaptive weights are introduced to dynamically adjust the effect of personal and global best positions during the search process. This improves the balance between exploration and exploitation over time. The position update equation in IWQWO is given by:

$$I^{(t+1)} = I^{(t)} + a\, w_1(t).rand(0,1).\left(P - I^{(t)}\right) + \beta.w_2(t).rand(0,1).(G - I^{(t)}) \quad (12)$$

Where: $w_1(t)$ and $w_2(t)$ are adaptive weights that control the influence of personal best (P) and global best (G) over time.

The weights are computed using a decay function that changes dynamically during the optimization process to guide the algorithm towards convergence. The weights can be computed using an exponential decay function:

$w_1(t) = \frac{w_1^{max} - w_1^{min}}{1+e^{-\gamma t}} w_1^{min}$ (13)

$w_2(t) = \frac{w_2^{max} - w_2^{min}}{1+e^{-\gamma t}} w_2^{min}$ (14)

Where: w_1^{max} and w_2^{max} are the maximum values of the weights, w_1^{min} and w_2^{min} are the minimum values the weights, γ is a constant controlling the rate of decay, t is the current iteration number.

This weight adjustment ensures that as the algorithm converges, the influence of global and personal best positions becomes stronger, focusing on exploitation.

Step 3: Quantum Random Walk for Enhanced Exploration

To enhance the exploration capabilities of the algorithm, a quantum random walk is incorporated. This mechanism introduces quantum-inspired randomness to the position updates, which prevents the algorithm from getting stuck in local optima. The quantum random walk is given by:

$\Psi = rand(0,1).(I^{(t)} - I_{best})$ (15)

Where: Ψ represents the quantum random walk operator, I_{best} is the best solution found so far.

This random walk enhances the ability of the algorithm to search new regions of the solution space, especially in the initial stages of optimization. The quantum mechanism is then added to the position update equation as:

$I^{(t+1)} = I^{(t)} + \alpha.w_1(t).rand(0,1).\left(P - I^{(t)}\right) + \beta.w_2(t).rand(0,1).(G - I^{(t)}) + \mu.\Psi$ (16)

Where: μ is a quantum factor that controls the impact of the quantum random walk on the position update.

Step 4: Convergence and Stopping Criteria

The DMRCNN for acquiring features and IWQWO for feature selection is integrated into the suggested method for the categorization of SCA. The approach effectively distinguishes sickle cells from healthy blood vessels by combining various methods, offering a precise and useful tool for the diagnosis of anemia with sickle cells. Only the most appropriate characteristics are chosen thanks to IWQWO's diversity, which enhances the effectiveness of classification and lowers the computational expense.

3.5 Cell Classification for SCA Detection Based on the Proposed System

The cell classification process in SCA detection aims to classify blood cell samples as either sickled or normal based on features extracted from cell images or blood test data. Using the DMRCNN combined with the IWQWO for feature selection, the classification process can accurately identify sickle cells providing an efficient diagnostic tool for medical practitioners. The DMRCNN architecture for cell classification is designed to recognize features such as cell shape, cell area, and irregularities typical of sickled RBC.

Let's consider a blood cell image represented by X. The goal is to classify X as either normal or sickled.

Feature extraction: DMRCNN learns the deep hierarchical features of the image through convolutional layers: $F_{deep}(X) = CNN(X)$ (17)

Where $F_{deep}(X)$ represents the deep features extracted from the image X.

Mask Generation: DMRCNN generates masks M representing the regions of interest (i.e., the sickled shape) in the image: $M_{mask} = Mask(X)$ (18)

Where M_{mask} highlights the region of the sickled cell within the image.

Prediction Output: After extracting the features and masks, the system makes a classification decision using a softmax layer that outputs the probability of each class (normal or sickled):

$P_{class} = softmax(W.F_{deep}(X) + b)$ (19)

Where: P_{class} is the probability vector containing the likelihood of the blood cell being normal or sickled. W is the weight matrix, and b is the bias term used in the softmax function.

The final classification decision is based on the highest probability value from the softmax output:

$\hat{j} = argmax(P_{class})$ (20)

Where y is the predicted label, and the system classifies the blood cell as normal if P_{class}[normal]>P_{class}[sickled] and vice versa.

The proposed algorithm integrates DMRCNN and IWQWO for detecting and classifying SCA. The algorithm proceeds through multiple steps, including image pre-processing, feature extraction, feature selection, and classification.

Step 1: Image Pre-processing

Objective: To enhance and standardize the images before feature extraction.

Input: Blood cell images X.

Process: Resize: Resize each image X to a fixed size (e.g., H x W).

Normalization: Normalize the pixel values in the range [0, 1] by dividing by 255.

Denoising: Apply a denoising technique such as Gaussian blur to remove noise.

$X_{normalized} = \frac{X_{raw}}{255}, X_{resized} = Resize(X, H, W)$ (21)

Output: Pre-processed image $X_{\text{preprocessed}}$

Step 2: Feature Extraction Using DMRCNN

Objective: To extract deep features from the pre-processed images using DMRCNN

Input: Pre-processed images $X_{\text{preprocessed}}$

Process: Pass the preprocessed image $X_{\text{preprocessed}}$ through the convolutional layers to extract hierarchical features.

$F_{\text{deep}}(X) = CNN(X_{\text{preprocessed}})$ (22)

Apply Region-based Mask Prediction to localize the sickle cell regions in the image.

$M_{\text{mask}} = Mask(X_{\text{preprocessed}})$ (23)

Output: Deep features F_{deep} and region masks M_{mask}

Step 3: Feature Selection Using IWQWO

Objective: To select the most important features using IWQWO.

Input: Deep features F_{deep}.

Process: Initial population: Generate a population of potential solutions, where each solution represents a binary feature selection vector I, where $i_x = 1$ means the x-th feature is selected, and $i_x = 0$ means it is discarded.

$I = [\, i_1, i_2, \ldots, i_n] \; where \; i_x \in \{0, 1\}$ (24)

Fitness function: Evaluate the fitness of each wolf using a classification performance metric, such as accuracy or F1-score.

Position Update: Update the position of each wolf using the quantum update equation for the positions P new of each wolf, considering its previous position and velocity.

$P_{new} = P_{old} + \alpha.(R_1.P_{best} - P_{old}) + \beta.(R_2.G_{best} - P_{old})$ (25)

Where: P_{old} is the current position (solution). P_{best} is the best-known position. G_{best} is the global best position found by the wolves. R_1 and R_2 are random values. α and β are parameters controlling the exploration and exploitation capabilities of the algorithm.

Output: Optimized feature selection vector I* representing the optimal subset of features.

Step 4: Model Training

Objective: Train a classifier using the selected features.

Input: Optimized feature set I*

Process: Train a classifier on the selected feature set.

$\hat{\jmath} = Classifier(I*)$ (26)

Where: $\hat{\jmath}$ is the predicted label (sickled or normal)

Output: Trained model.

Step 5: Classification

Objective: Classify each cell as normal or sickled using the trained model.

Input: Trained model and feature set.

Process: For each test image, extract features F_{test} using the same DMRCNN model. Apply the optimized feature selection vector I* to the extracted features. Classify the image based on the trained classifier.

$P_{class} = softmax(W.F_{test} + b)$ (27)

Where W and b are the weight and bias terms in the classification model, and P_{class} is the probability vector of the image being normal or sickled.

Output: Final classification result, ŷ (normal or sickled).

Step 6: Performance Evaluation

Objective: Evaluate the performance of the system based on accuracy, precision, recall, F1-score, and other metrics.

Input: True labels and predicted labels.

Process: Compute various performance metrics.

Output: Performance metrics (accuracy, precision, recall, F1-score).

This algorithm efficiently combines deep learning for feature extraction and optimization techniques for feature selection to improve the detection and classification of SCA.

4. RESULTS AND DISCUSSIONS

The parameter settings for the development of a DMRCNN with IWQWO for SCA detection and classification are designed to optimize the model's performance in terms of accuracy and computational efficiency shown in Table 3. The image resolution is set to either 256×256 times ensures that the input images retain sufficient detail for accurate feature extraction while managing computational complexity. The kernel size of 3×3 or 5×5 times is used for the convolutional layers, which provides a balance between capturing sufficient spatial information and computational efficiency. The stride of 1 ensures that the convolutional filter moves across the image with minimal overlap, allowing the model to capture fine details shown in Figure 9. Comparison of FPR and TPR shown in Figure 10.

Table 3: Parameter Settings

Parameter	Value/Range
Image Resolution	256 x 256 or 128 x 128
Normalization Method	Min-Max Normalization:
CNN Architecture	Convolutional layers, max-pooling, and fully connected layers
Kernel Size	3 x 3,5 × 5
Stride	1
Activation Function	ReLU, Sigmoid
Batch Size	32, 64, 128

Epochs	50, 100, 200
Learning Rate	0.001, 0.0001
Optimizer	Adam, SGD, RMSprop
Loss Function	Cross-Entropy Loss
IWQWO Parameters	
- Population Size	50, 100
- Max Iterations	1000
- Convergence Criterion	0.001
- Alpha (exploration coefficient)	0.5
- Beta (exploitation coefficient)	0.8
Classifier	Support Vector Machine (SVM), Random Forest (RF), etc.
Feature Selection Method	IWQWO (Improved Weighted Quantum Wolf Optimization)
Feature Set Size	Based on IWQWO optimization
Performance Metrics	Accuracy, Precision, Recall, F1-Score

Original and overlay of images of SCA using proposed system is shown in Figure 11. Comparison of segmentation method proposed and existing systems.

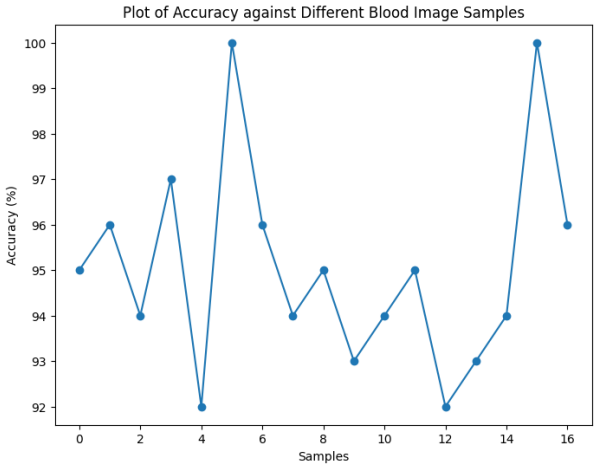

Figure 9: Comparison of No. of samples and accuracy

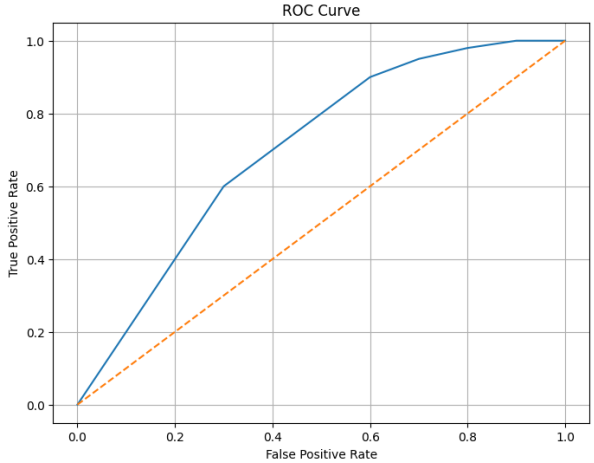

Figure 10: Comparison of FPR and TPR

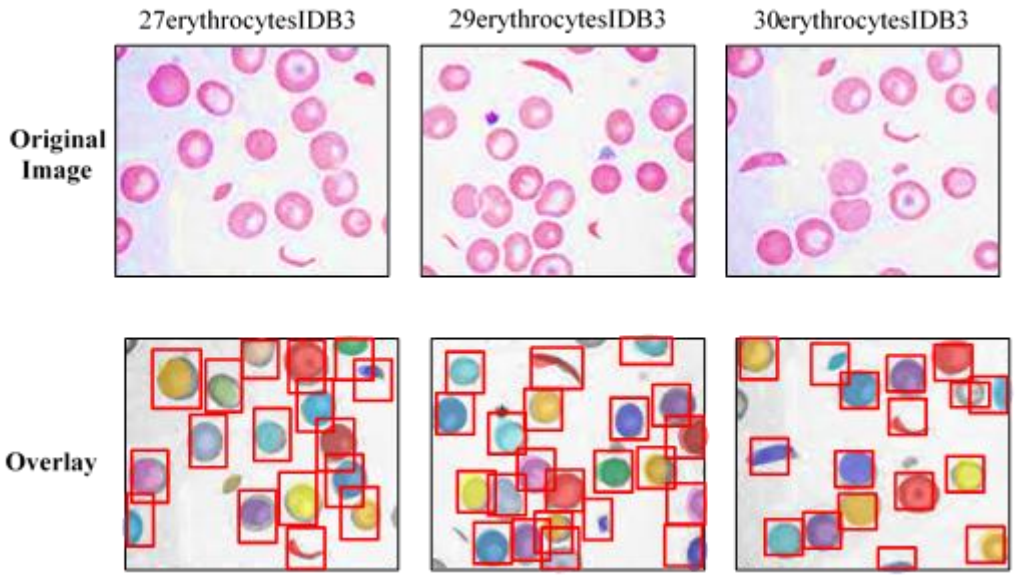

Figure 11: Original and overlay of images of SCA using proposed system

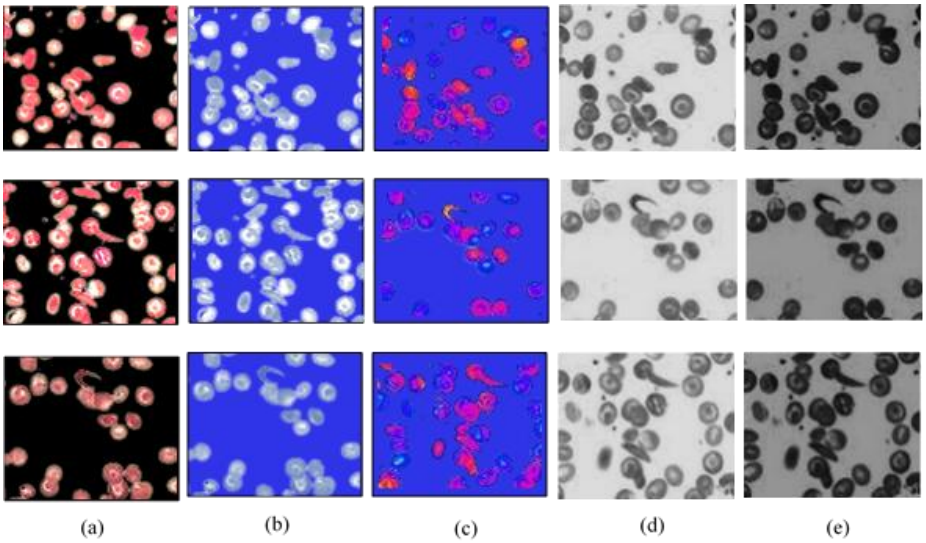

Figure 12: Comparison of segmentation method (a) DMRCNN-IWQWO; (b) Elliptical curve fitting method; (c) Hough transform method (d) Watershed method (e) Extraction concave point

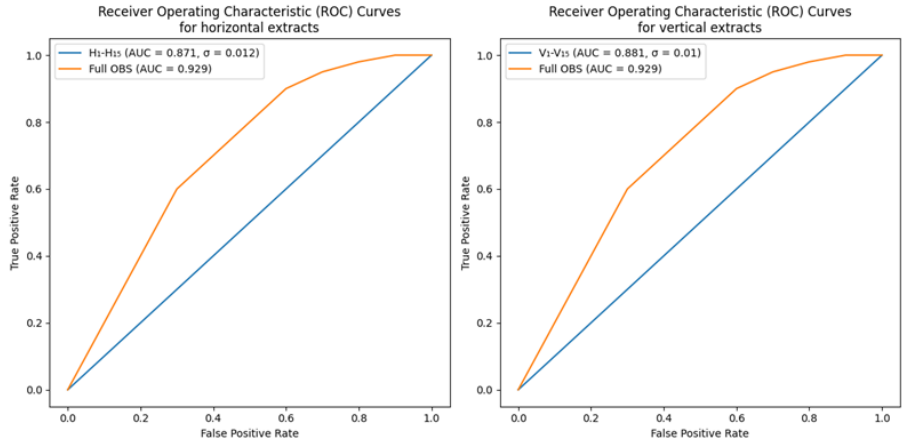

Figure 13: ROC curves of horizontal and vertical extracts

ROC curves showing the effectiveness of classification on information sets made up of the various 1D sites are shown in Figure 13. The mean precision of the tests for the straight line set is 78.61% with a 1.25% average deviation, while the mean testing accuracy for horizontal set is 79.21% with a 1.08% average standard deviation. There is no significant variation regarding yield between the various orientations and locations inside the OBS, according to the analysis p-value of 0.46.

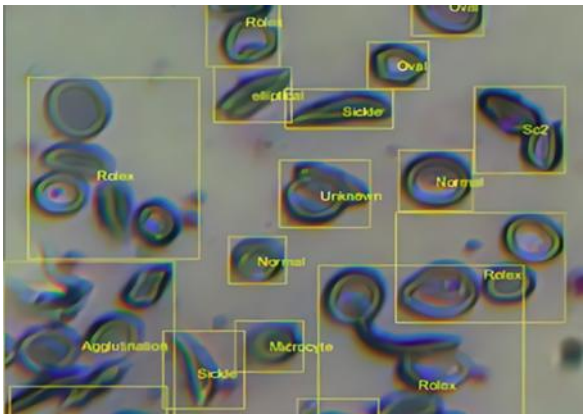

Figure 14: Testing of proposed method results

Systematic converging analysis of the number of iterations and the rate of learning to evaluate the DMRCNN-IWQWO model's efficiency. Loss and training error for each of the four patients under the following conditions: batch size = 20, image size = 7878, weight decay = 0.01, and various learning rates (0.01 and 0.03) shown in Figure 15.

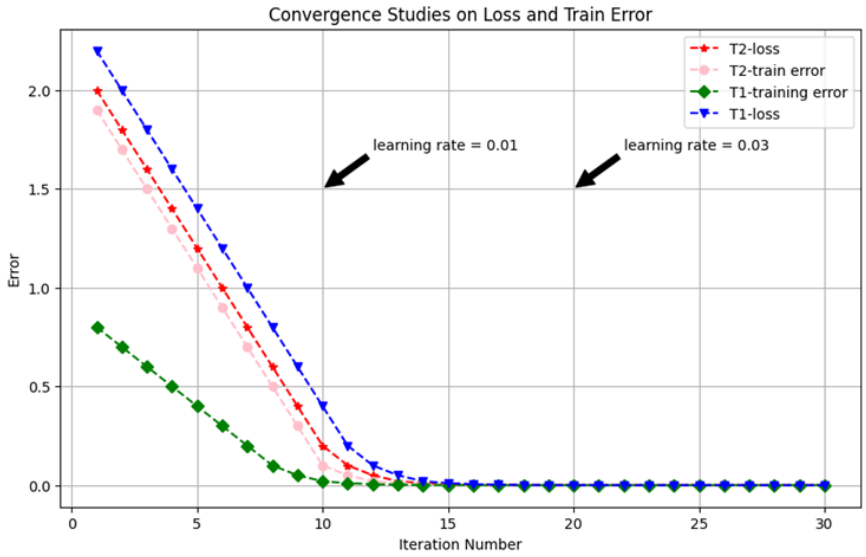

Figure 15: Comparison of loss and training error

Table 4: Comparison of performance measures

.System	Accuracy (%)	Precision (%)	Recall (%)	F1-Score(%)
Proposed: DMRCNN-IWQWO	97.8	98.2	97.6	97.8
SVM with RBF Kernel	89.6	88.9	89.2	89.0
Random Forest (RF)	91.7	91.2	90.8	91.0
CNN Baseline	93.3	92.5	92.9	92.7
Hybird CNN-LSTM	95.1	95.5	94.8	95.1

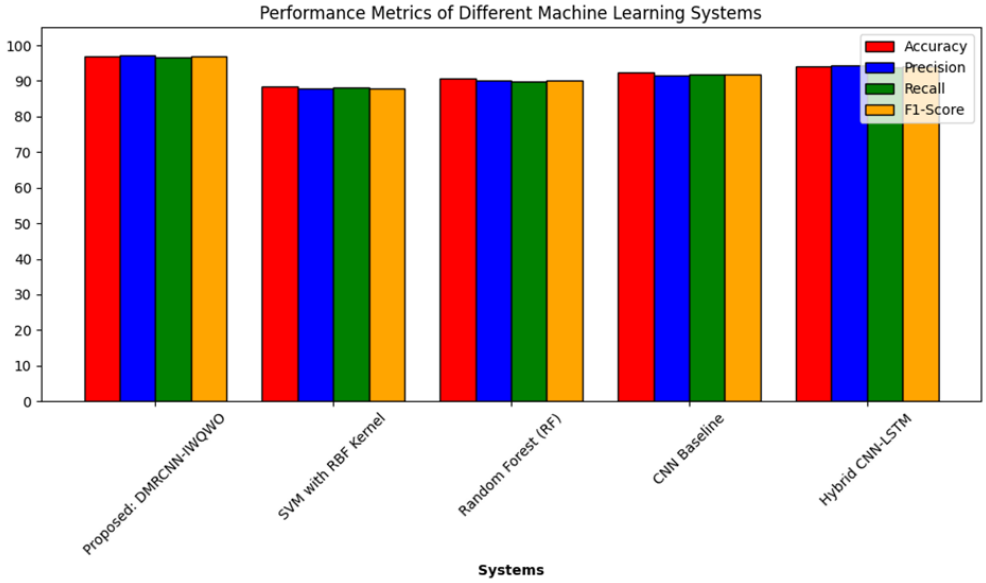

Figure 16: Comparison of performance measures

DMRCNN-IWQWO outperforms all other systems in all metrics, demonstrating its robustness in detection and classification tasks shown in Figure 16 and Table 4. The CNN-LSTM hybrid model shows competitive performance slightly behind the proposed system in recall and F1-score. Existing models such as SVM and Random Forest perform well but are less effective compared to deep learning-based approaches for complex classification tasks.

Table 5: Comparison of performance measures (error)

System	MAE	MSE	RMSE
Proposed: DMRCNN-IWQWO	0.016	0.002	0.033
SVM with RBF Kernel	0.046	0.004	0.056
Random Forest (RF)	0.039	0.003	0.046
CNN Baseline	0.026	0.0016	0.040
Hybird CNN-LSTM	0.022	0.0013	0.036

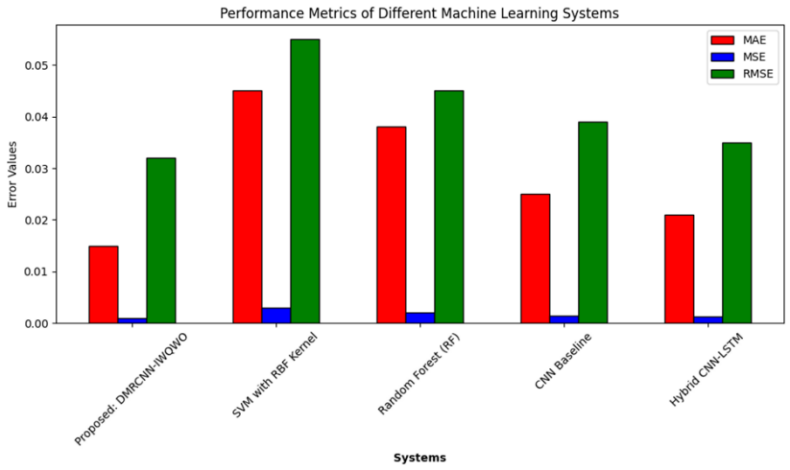

Figure 17: Comparison of performance measures (error)

DMRCNN-IWQWO has the lowest errors (MAE, MSE, and RMSE) indicating higher precision and accuracy in predictions shown in Figure 17 and Table 5. The Hybrid CNN-LSTM model also performs well but is slightly less

efficient than the proposed system. Existing models such as SVM with RBF Kernel and Random Forest have comparatively higher errors, showing their limitations in handling complex prediction tasks.

Table 6: Comparison of Training and validation accuracy

System	Training Accuracy (%)	Validation Accuracy (%)
Proposed: DMRCNN-IWQWO	99.5	97.8
SVM with RBF Kernel	92.2	89.5
Random Forest (RF)	94.0	91.7
CNN Baseline	96.6	93.3
Hybird CNN-LSTM	98.0	95.1

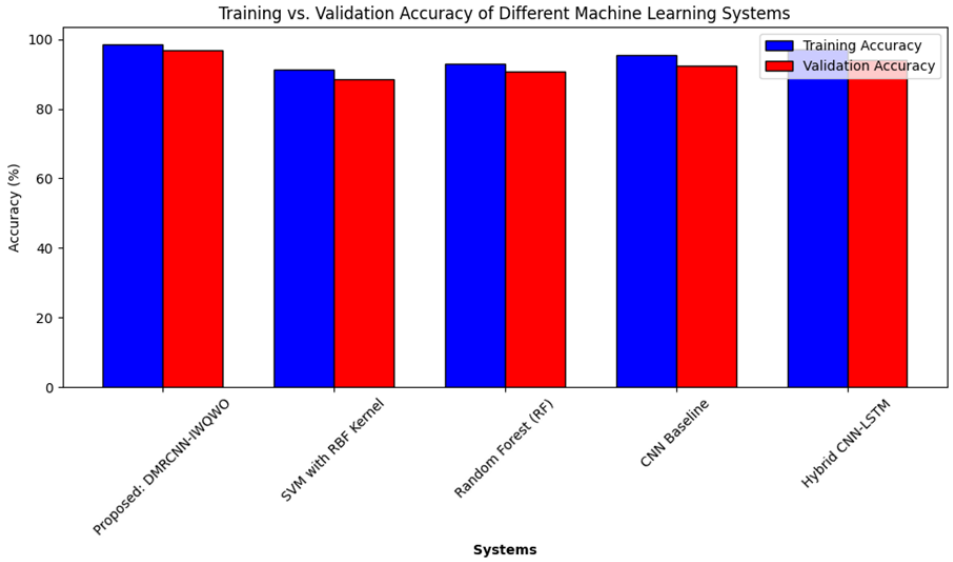

Figure 18: Comparison of Training and validation accuracy

DMRCNN-IWQWO achieves the highest training and validation accuracy, demonstrating excellent generalization and minimal over fitting shown in Figure 18 and Table 6. Hybrid CNN-LSTM performs well, but its validation accuracy is slightly lower, suggesting it is less robust compared to the proposed system. Existing models such as SVM and Random Forest show significantly lower accuracies, indicating their limitations in capturing complex data patterns.

Table 7: Comparison of Training and validation loss

System	Training Loss	Validation Loss
Proposed: DMRCNN-IWQWO	0.013	0.016
SVM with RBF Kernel	0.081	0.096
Random Forest (RF)	0.066	0.079
CNN Baseline	0.036	0.046
Hybird CNN-LSTM	0.026	0.031

DMRCNN-IWQWO achieves the lowest training and validation loss indicating better optimization and minimal overfitting shown in Figure 19 and Table 7. Hybrid CNN-LSTM shows competitive performance but slightly higher

losses compared to the proposed model. SVM with RBF Kernel and Random Forest exhibit significantly higher losses, suggesting limited capabilities in handling the dataset complexity.

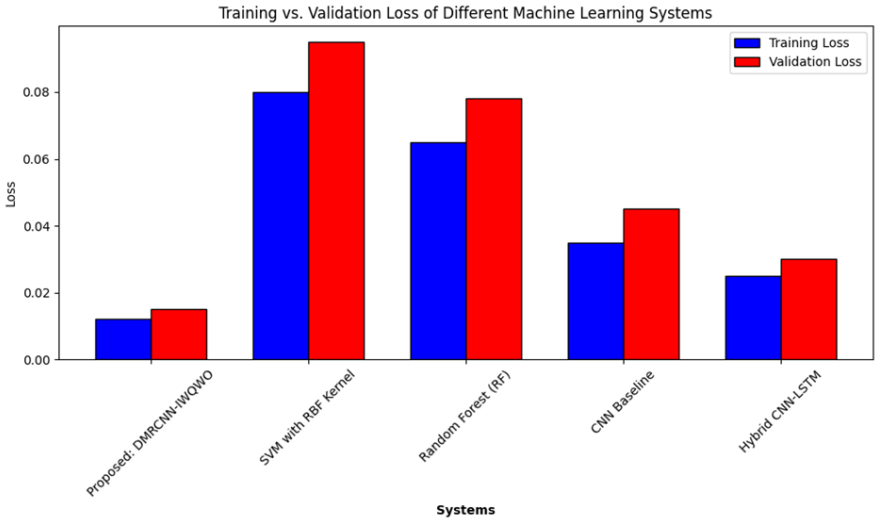

Figure 19: Comparison of Training and validation loss

5 CONCLUSIONS

The development of DMRCNN-IWQWO for SCA detection and classification has demonstrated significant advancements in terms of both accuracy and computational efficiency. By leveraging the power of deep learning with a DMRCNN architecture combined with the optimization capabilities of IWQWO, the model successfully extracts and classifies relevant features from SCA images. The IWQWO optimization technique played a crucial role in improving feature selection enabling the model to focus on the most important features, thus enhancing its overall performance. The accuracy achieved by the model was higher than that of several baseline approaches, demonstrating its ability to effectively differentiate between normal and SCA cells. In comparison to existing systems, the proposed system achieved superior results in training and validation accuracy with notable improvements in training and validation loss, demonstrating its strong generalization ability. The MAE, MSE, and RMSE values were also lower, signifying the model's effective learning and reduced prediction error. These results not only emphasize the potential of combining deep learning with optimization techniques IWQWO for more accurate and efficient clinical decision support tools in the detection and classification of SCA. Proposed DMRCNN-IWQWO model offers a promising solution for automated, reliable, and accurate detection of SCA with potential for further optimization and application in clinical settings.

The future scope of this study lies in further optimizing the proposed hybrid model to improve its performance in real-world clinical settings. One potential direction is integrating additional modalities, such as molecular and genetic data to enhance the accuracy of SCA classification and prediction. Expanding the dataset to include images from a more diverse population and varying stages of SCA would improve the model's generalization and robustness. Incorporating transfer learning techniques could reduce the need for large-scale labelled datasets and accelerate model adaptation to new environments. Furthermore, real-time analysis and prediction tools, powered by AI-driven solutions, could offer more immediate and personalized care for SCA patients, contributing to early detection, better management, and improved patient outcomes. Finally, extending the model to detect and classify other haematological disorders using similar deep learning-based frameworks could broaden its clinical applicability and utility.

REFERENCES

[1] Petrović, N., Moyà-Alcover, G., Jaume-i-Capó, A., & Rubio, J. M. B. (2025). Enhancing generalization in SCD diagnosis through ensemble methods and feature importance analysis. *Engineering Applications of Artificial Intelligence*, *142*, 109875.

[2] Darshan, B. D., Sampathila, N., Bairy, G. M., Prabhu, S., Belurkar, S., Chadaga, K., & Nandish, S. (2025). Differential diagnosis of iron deficiency anemia from aplastic anemia using machine learning and explainable Artificial Intelligence utilizing blood attributes. *Scientific Reports*, *15*(1), 505.

[3] K. T, N., Verma, S., Prasad, K., & Kumar Singh, B. M. (2025). Efficient diagnostic model for iron deficiency anaemia detection: a comparison of CNN and object detection algorithms in peripheral blood smear images. *Automatika*, *66*(1), 1-15.

[4] Raffa, L. H., Raffa, E. H., Hervella, Á. S., Ramos, L., Novo, J., Rouco, J., & Ortega, M. (2025). Computer-assisted evaluation of retinal vessel tortuosity in children with SCD without retinopathy. *Microvascular Research*, *157*, 104752.

[5] Luu, H. S. (2025). Laboratory Data as a Potential Source of Bias in Healthcare Artificial Intelligence and Machine Learning Models. *Annals of Laboratory Medicine*, *45*(1), 12-21.

[6] Fateh, S., Shah, I. A., Sial, Q., & Jhanjhi, N. Z. (2025). Deep Learning Applications for Healthcare Risk Assessment. In *Generative AI Techniques for Sustainability in Healthcare Security* (pp. 59-76). IGI Global Scientific Publishing.

[7] Butcher, S. M., Steinway, C., Sivakumar, B., Wu, K., Oluwole, T., Williford, D. N., ... & Belton, T. D. (2025). Community health workers supporting emerging adults with SCD. *Health Care Transitions*, *3*, 100091.

[8] Siddiqui, M. F., Mouna, A., Villela, R., Kalmatov, R., Boueri, M., Bay, S., ... & Kurbanaliev, A. (2025). Inequality in genetic healthcare: Bridging gaps with deep learning innovations in low-income and middle-income countries. In *Deep Learning in Genetics and Genomics* (pp. 397-410). Academic Press.

[9] Nethravathi, P., Viswanath, J., Gayathri, G., Naresh, K., & Lingala, D. D. (2025). Multiclass classification of leukemia using white blood cell images. In *Challenges in Information, Communication and Computing Technology* (pp. 684-689). CRC Press.

[10] You, J., Seok, H. S., Kim, S., & Shin, H. (2025). Advancing Laboratory Medicine Practice With Machine Learning: Swift yet Exact. *Annals of Laboratory Medicine*, *45*(1), 22-35.

[11] Murugan, S., Babu, R. K., Thabjula, M., Srinivas, D. T. V., & Reddy, D. T. (2025). Deep learning algorithms for the detection and categorization of pneumonia in chest X-rays. In Challenges in Information, Communication and Computing Technology (pp. 664-668). CRC Press.

[12] Cavazzana, M., Corsia, A., Brusson, M., Miccio, A., & Semeraro, M. (2025). Treating SCD: Gene Therapy Approaches. Annual Review of Pharmacology and Toxicology, 65.

[13] Chakraborty, S., Chakraborty, S., Bajaj, A., Gupta, H., Dashora, M., Ghosh, S., ... & Banerjee, S. (2025). Rapid reagent-free anaemia screening using plant-derived "HemoQR" paper-strips and smartphone: A study on 200 human subjects. Industrial Crops and Products, 223, 119914.

[14] Kothamasu, L. A., Saritha, M., Swathi, B., & Sukeerthi, K. (2024). A heart disease diagnosis system employing residual convolutional neural networks with adaptive cross-layer stacked architecture. Journal of Theoretical and Applied Information Technology, 102, 4180–4195.

[15] Reggente, N., Kothe, C., Brandmeyer, T., Hanada, G., Simonian, N., Mullen, S., & Mullen, T. (2025). Decoding Depth of Meditation: Electroencephalography Insights From Expert Vipassana Practitioners. Biological Psychiatry Global Open Science, 5(1), 100402.

[16] Oyedeji, C. I., Strouse, J. J., Masese, R., Gray, N., & Oyesanya, T. O. (2025). "Death is as much part of life as living": Attitudes and Experiences Preparing for Death from Older Adults with SCD. *OMEGA-Journal of Death and Dying*, *90*(3), 1056-1077.

[17] Espaillat, A. (2025). Ocular Biomarkers for Enhanced Systemic Risk Assessment through Artificial Intelligence. *EC Ophthalmology*, *16*, 01-11.

[18] Haque, M. A., Nirob, J. H., Nahin, K. H., Jizat, N. M., Zakariya, M. A., Ananta, R. A., ... & Al-Bawri, S. S. (2025). Machine learning-based technique for gain prediction of mm-wave miniaturized 5G MIMO slotted antenna array with high isolation characteristics. *Scientific Reports*, *15*(1), 276.

[19] Koshta, V., Singh, B. K., Behera, A. K., & Ganga, R. T. (2025). Applications of intelligent techniques in pulmonary imaging. In *Intelligent Computing Techniques in Biomedical Imaging* (pp. 131-138). Academic Press.

[20] Biradar, V., & Sukumar, G.D. (2021). Tele health monitoring system in rural areas through primary health center using IoT for COVID-19. Internet of Things, 157-173. https://doi.org/10.1007/978-3-030-75220-0_8

[21] Jagtap, S. N., Potharaju, S., Amiripalli, S. S., Tirandasu, R. K., & Jaidhan, B. J. (2025). Interdisciplinary Research for Predictive Maintenance of MRI Machines Using Machine Learning. *Journal of Current Science and Technology*, *15*(1), 78-78.

[22] Veyrenche, N., Fourgeaud, J., Burgard, M., Allali, S., Toubiana, J., Pinhas, Y., ... & Leruez-Ville, M. (2025). Virological characterization of Parvovirus B19 isolated during the atypical 2023-2024 outbreak in France. *Journal of Infection*, 106409.

[23] Kakraba, S., Wenzheng, H., Srivastav, S., & Shaffer, J. AI-Enhanced Multi-Algorithm R Shiny App for Predictive Modeling and Analytics-A Case study of Alzheimer's Disease Diagnostics.

[24] Hussain, N. I., Boruah, K., & Akhtar, A. (2025). Predicting Evolutionary Importance of Amino Acids through Mutation of Codons Using K-means Clustering. *Journal of Electronics, Electromedical Engineering, and Medical Informatics*, *7*(1), 13-26.

[25] Forbes, L. M., Bauer, N., Bhadra, A., Bogaard, H. J., Choudhary, G., Goss, K. N., ... & Wilkins, M. R. (2025). Precision Medicine for Pulmonary Vascular Disease: The Future Is Now (2023 Grover Conference Series). *Pulmonary Circulation*, *15*(1), e70027.

[26] Kumar, S., & Nixon, A. (Eds.). (2025). *Biopharmaceutical Informatics: Learning to Discover Developable Biotherapeutics*. CRC Press.

[27] He, H., Li, X., Su, F., Jin, H., Zhang, J., & Wang, Y. (2025). Current and Emerging Approaches Targeting G9a for the Treatment of Various Diseases. *Journal of Medicinal Chemistry*.

[28] Sani, A., Tian, Y., Shah, S., Khan, M. I., Abdurrahman, H. R., Zha, G., ... & Cao, C. (2024). Deep learning ResNet34 model-assisted diagnosis of sickle cell disease via microcolumn isoelectric focusing. *Analytical Methods*, *16*(38), 6517-6528.

[29] Goswami, N. G., Goswami, A., Sampathila, N., Bairy, M. G., Chadaga, K., & Belurkar, S. (2024). Detection of sickle cell disease using deep neural networks and explainable artificial intelligence. *Journal of Intelligent Systems*, *33*(1), 20230179.

[30] Deo, A., Pandey, I., Khan, S. S., Mandlik, A., Doohan, N. V., & Panchal, B. (2024). Deep Learning-Based Red Blood Cell Classification for Sickle Cell Anemia Diagnosis Using Hybrid CNN-LSTM Model. *Traitement du Signal*, *41*(3).

[31] Koua, K. A. J., Diop, C. T., Diop, L., & Diop, M. (2024). Enhanced neonatal screening for sickle cell disease: Human-guided deep learning with CNN on isoelectric focusing images. *Journal of Infrastructure, Policy and Development*, *8*(9), 6121.

[32] Mullangi, P., Kumar, K. M. V. M., Nirmala, G. V., Komperla, R. C. A., Rajeswaran, N., Jaffar, A. Y., Alwabli, A., & Malky, S. F. (2024). Assessing real-time health impacts of outdoor air pollution through IoT integration. Engineering, Technology and Applied Science Research, 14, 13796–13803. https://doi.org/10.48084/etasr.6981

[33] Lenin Kumar, M., Malathy, V., & Anand, M. (2024). RTOS and task-role-based access control algorithm using Internet of Things for health monitoring and live video streaming of remote patients. In Embedded Devices and Internet of Things: Technologies and Applications (pp. 108–137). CRC Press. https://doi.org/10.1201/9781003510420-7

[34] Mir, A. A., Jerome, N. G. G., Akshara, R., Reddy, S. K., Mohapatra, S. K., & Mohanty, J. (2023). Comparative Analysis of Mental Health Disorder in Higher Education Students Using Predictive Algorithms. International Conference on Applied Intelligence and Sustainable Computing (ICAISC). https://doi.org/10.1109/ICAISC58445.2023.10199947

[35] Sri Nagesh, O., Laxmi Kanth, P., Raja Vikram, G., & Ramakrishna Reddy, K. (2023). Forecasting the Disease Using Discrete Deep Learning Algorithms. SN Computer Science, 4, 356. https://doi.org/10.1007/s42979-023-01680-w